Title: Molecular design approach managing molecular orbital superposition for high efficiency without color shift in thermally activated delayed fluorescent organic light-emitting diodes

Authors: Mounggon Kim, Ph.D.; Seong-Jun Yoon, Ph.D.; Si Hyun Han; Ramin Ansari; John Kieffer, Ph.D.; Jun Yeob Lee, Ph.D.; Jinsang Kim, Ph.D.

To be cited as: 10.1002/chem.201805616

Link to VoR: https://doi.org/10.1002/chem.201805616

Molecular design approach managing molecular orbital superposition for high efficiency without color shift in thermally activated delayed fluorescent organic light-emitting diodes

Mounggon Kim[1+], Seong-Jun Yoon[1+], Si Hyun Han[2+], Ramin Ansari[3], John Kieffer[1], Jun Yeob Lee*[2] and Jinsang Kim*[1]

* Corresponding authors

[1]M. Kim, S.-J. Yoon, Prof. J. Kieffer and Prof. J. Kim

Department of Materials Science and Engineering, University of Michigan, Ann Arbor, USA

E-mail: jinsang@umich.edu

[2]S. H. Han and Prof. J. Y. Lee

School of Chemical Engineering, Sungkyunkwan University

2066, Seobu-ro, Jangan-gu, Suwon, Gyeonggi, 440-746, Korea

E-mail: leej17@skku.edu

[3]R. Ansari

Department of Chemical Engineering, University of Michigan, Ann Arbor, USA

+M. Kim, S.-J. Yoon, and S. H. Han contributed equally to this work.

Abstract

Molecular design principle of thermally activated delayed fluorescent (TADF) emitters having a high quantum efficiency and a color tuning capability was investigated by synthesizing three TADF emitters with donors at different positions of a benzonitrile acceptor. The position rendering a large overlap between the highest occupied molecular orbital (HOMO) and the lowest unoccupied molecular orbital (LUMO) enhances the quantum efficiency of the TADF emitter. Regarding the orbital overlap donor attachments at 2 and 6 positions of the benzonitrile were more beneficial than 3 and 5 substitutions. Moreover, an additional attachment of a weak donor at 4 position further increased the quantum efficiency without decreasing the emission energy. Therefore, the molecular design strategy of substituting strong donors at the positions allowing a large molecular orbital overlap and an extra weak donor is a good approach for both a high quantum efficiency and a slightly increased emission energy.

Keywords: orbital superposition, direct position, non-linker, TADF, OLEDs

Introduction

There has been a great progress in the external quantum efficiency (EQE) of organic light-emitting diodes (OLEDs) for the last 20 years, which was mostly led by phosphorescent OLED technology enabling 100% triplet exciton harvesting efficiency.[1-7] However, the usage of precious Ir in the molecular structure is not cost-effective, which inspired the development of purely organic based thermally activated delayed fluorescence (TADF)[8-16] and metal-free organic phosphors[17-20] as an alternative to the organometallic phosphors.

Numerous TADF materials have been devised based on basic design rules to manipulate the singlet transition process and triplet exciton up-conversion process. The molecular design approach for the efficient singlet transition process and triplet up-conversion process is self-contradictory because the first process requires a large HOMO-LUMO overlap, whereas the second process demands a large HOMO-LUMO separation. However, the conflicting requirements can be resolved by rational design of TADF chemical structure. The most common design is based on a donor-acceptor chemical platform, particularly, a multiple donor type structure[8, 12, 21-24], a dual emitting core structure[25-27], and a multiple resonance type donor-acceptor structure[28]. These chemical approaches are proven to be effective by demonstrating a high EQE over 20% and a high photoluminescence (PL) quantum yield close to 100%. Especially, the multiple donor type designs, such as (4s,6s)-2,4,5,6-tetra(9H-carbazol-9-yl) isophthalonitrile (4CzIPN)[8,29-32] and 9,9',9''-(5-(4,6-diphenyl-1,3,5-triazin-2-yl)benzene-1,2,3-triyl)tris(9H-carbazole) (TCzTrz)[33], are most popular as the main building block of the TADF emitters. Inclusion of multiple donors in the TADF molecules is known to increase the HOMO-LUMO overlap and to reduce the singlet-triplet energy gap (ΔE_{ST}). Consequently, a high singlet transition efficiency and a reverse intersystem crossing (RISC) efficiency are simultaneously achievable in those molecules. However, one of unanswered

questions is the effect of the donor position in the molecular structure on the light-emitting performance although the multiple donors themselves enhance the light emission efficiency. The substitution position effects of donor have been reported for host materials[34,35] and TADF emitters containing a single donor[36,37]. However, reports discussing the donor position effect in the TADF emitters with multiple donors are very rare, and there is no systematic investigation. Moreover, additional donor unit is prone to red-shift the wavelength of the resulting TADF molecule, which makes it challenging to develop high efficiency TADF emitters with a short emission wavelength. Therefore, it is meaningful to explore the molecular design approach for enhancing the efficiency while keeping the same emission spectrum.

Herein, we designed and synthesized TADF emitters composed of multiple phenoxazine donors and a benzonitrile acceptor. Very recently, Adachi and coworkers reported deep-blue TADF emitters containing multiple carbazole donors and a benzonitrile acceptor, in which the donor strength of the substituted carbazole was shown to play an important role in the TADF properties but the connection position of carbazole donors was not investigated.[38] In this work, the connection position of the phenoxazine donors to the benzonitrile acceptor was managed and the effect of the donor position on the TADF characteristics was examined. Comparison of the three TADF emitters, 2,6-di(10H-phenoxazin-10-yl)benzonitrile (o-CNPhe), 3,5-di(10H-phenoxazin-10-yl)benzonitrile (m-CNPhe), and 4-(diphenylamino)-2,6-di(10H-phenoxazin-10-yl)benzonitrile (o-CNPheAm), indicated that 2 and 6 substitution of donors is more effective than 3 and 5 substitution in enhancing EQE of the TADF devices. Moreover, additional attachment of a relatively weak diphenylamine donor at 4 position of the benzonitrile further increased the EQE of the devices without lowering the emission energy. The demonstrated substitution position dependent EQE of the TADF devices is well correlated with the molecular orbital superposition of the TADF emitters.

Result and discussion

The three TADF molecules, o-CNPhe, m-CNPhe, and o-CNPheAm, have a benzonitrile acceptor and phenoxazine donors or a mixed donor of phenoxazine and diphenylamine. The o-CNPhe and m-CNPhe are similar in that they have two phenoxazine donors attached to the benzonitrile, but at different substitution positions (2 and 6 in o-CNPhe, 3 and 5 in m-CNPhe). The o-CNPheAm has an additional diphenylamine donor at 4 position of the o-CNPhe. The three emitters are designed so as to study the effect of the substitution position linked to the molecular orbital superposition on the TADF emission characteristics.

Synthetic scheme of o-CNPhe, m-CNPhe, and o-CNPheAm is shown in **Scheme. 1**. The three molecules were simply prepared by 1-step or 2-step reaction procedures. Final yields of o-CNPhe, m-CNPhe, and o-CNPheAm were 82%, 72% and 54%, respectively. All molecules were purified using a vacuum train sublimation procedure to have over 99% purity (see Figure S1 in the Supporting Information (SI) for the purity confirmation).

The HOMO and LUMO distribution were calculated using basic set of B3LYP/6-311+G** in the gaussian 09 program and the molecular orbital calculation outputs of o-CNPhe, m-CNPhe, and o-CNPheAm are shown in **Figure 1** together with the calculation results of the benzonitrile acceptor (see Table S1 in the SI for the summary of TD-DFT calculation). As the benzonitrile is an acceptor of the TADF emitters, the LUMO distribution is important for the TADF emission characteristics. The LUMO calculation results show that the LUMO is localized on 1 and 4 positions of the phenyl ring, and the 2 and 6 positions have relatively higher LUMO density than 3 and 5 positions. Comparing the 1 and 4 positions, 1 position has rather large contribution to the LUMO density. In the design of the TADF emitters, the HOMO and LUMO overlap is critical to the radiative transition process from the singlet

excited state to the ground state. The HOMO and LUMO overlap is extensive when the donors are placed at the substitution positions having a strong LUMO character. Therefore, the molecular orbital picture of benzonitrile suggests that the substitution of donors at 2, 6, and 4 positions of benzonitrile would increase the radiative transition probability.

The HOMO and LUMO pictures of o-CNPhe and m-CNPhe indicate that the HOMO-LUMO superposition mostly occurs on the benzonitrile acceptor. The HOMO-LUMO overlap of o-CNPhe is possible at 2, and 6 positions of benzonitrile, whereas that of m-CNPhe is enabled at 3, and 5 positions of benzonitrile. It can be presumed from the molecular orbital data that the o-CNPhe would have better HOMO-LUMO overlap for efficient singlet emission than m-CNPhe. In the case of o-CNPheAm, the HOMO and LUMO distribution of the frontier orbital of o-CNPheAm was similar to that of o-CNPhe, but there is additional contribution to the HOMO-LUMO overlap by the triphenylamine unit at 4- position. Therefore, the o-CNPheAm is anticipated to perform better than the other two emitters in the singlet emission process.

Photophysical characterization of the TADF emitters is important to correlate the structure of TADF emitters with light absorption and emission properties. Ultraviolet-visible (UV-Vis) and photoluminescence (PL) characterization of o-CNPhe, m-CNPhe, and o-CNPheAm are compared in **Figure 2(a)**. UV-Vis absorption spectra of the o-CNPheAm reflected its extended conjugation by showing red-shifted absorption peak and a strong charge transfer (CT) character by exhibiting absorption over 350 nm owing to the additional diphenyl amine at 4- position. The maximum absorption coefficients (ε) of the three molecules were 0.94 x 10^5 M^{-1} cm^{-1} for o-CNPhe, 0.87 x 10^5 M^{-1} cm^{-1} for m-CNPhe, and 0.92 x 10^5 M^{-1} cm^{-1} for o-CNPheAm, respectively.

Room temperature PL (fluorescence) and low temperature PL (phosphorescence)[38,39] of the

three TADF emitters were measured to characterize the emission properties and the singlet/triplet energy (**Figure 2(b)**). The singlet energy of o-CNPhe, m-CNPhe, and o-CNPheAm corresponding to the emission from the CT singlet excited state was estimated to be 2.80, 2.82, and 2.82 eV, respectively, from the onset energy of the fluorescence. The singlet energy of o-CNPheAm was not decreased although an additional diphenylamine donor was substituted at 4- position because the diphenylamine is a relatively weak donor compared to phenoxazine. The donor character is dominated by the phenoxazine donor and the diphenylamine donor has negligible effect on the singlet energy. The singlet energy was rather slightly increased due to the weakened acceptor character of benzonitrile by diphenylamine. The triplet energy of o-CNPhe, m-CNPhe, and o-CNPheAm was calculated to be 2.80, 2.80 and 2.76 eV, respectively, from the onset energy of phosphorescence. The triplet energy of o-CNPheAm was relatively low because of the diphenyl donor at 4- position. The ΔE_{ST} of o-CNPhe, m-CNPhe, and o-CNPheAm was 0.00, 0.02, and 0.06 eV, respectively.[38,40] Photophysical properties of TADF emitters are summarized in **Table 1**.

Transient PL decay curves of TADF emitters are shown in **Figure 3**. The delayed fluorescence lifetime of o-CNPhe, m-CNPhe, and o-CNPheAm doped films was 2.4, 4.6 and 8.9 μs, respectively, which is correlated very well with their ΔE_{ST} value. PLQY of o-CNPhe, m-CNPhe, and o-CNPheAm doped films was 66.4, 49.8, and 81.0% under nitrogen, respectively. o-CNPhe performs better than m-CNPhe as anticipated based on their molecular orbital distribution, and o-CNPheAm was superior to o-CNPhe due to the additional diphenylamine donor and consequentially expanded molecular orbital overlap. In the literature, we could find a TADF emitter composed of two phenoxazine donors and a phthalonitrile acceptor, which is structurally similar to our TADF molecules.[41] The reported much lower PLQY of 6.4% of that emitter also supports that the substitutional position of multiple donors and acceptors is crucial for the TADF properties.

The **Figure 4** compares EQE of the o-CNPhe, m-CNPhe, and o-CNPheAm devices at a doping concentration of 10%. The host material of the devices was a mixed host of 1,3-bis(N-carbazolyl)benzene (mCP) and 1,3,5-tris(1-phenyl-1H-benzimidazol-2-yl)benzene (TPBi). Current density, luminance, and voltage data are presented in the supporting information (**Figure S3**). The o-CNPheAm device showed the highest EQE of 12.0% among the three TADF devices, while o-CNPhe and m-CNPhe devices provided maximum EQEs of 9.0% and 7.7%, respectively. This result agrees with the PLQY of the three TADF emitters, suggesting that the proper substitution point of donor moieties are the LUMO-rich positions of the acceptor for a large HOMO-LUMO overlap favorable for radiative transition process. The efficiency roll-off of o-CNPhe and m-CNPhe is better than o-CNPheAm because of relatively short lifetime.

The electroluminescence (EL) spectra of the TADF devices are presented in **Figure 5**. The λ_{max} of the EL spectra match well with the trend of the relative PL λ_{max}. The EL λ_{max} of o-CNPhe, m-CNPhe, and o-CNPheAm devices was 515, 511, and 509 nm, respectively. Slightly blue shifted emission was observed in the o-CNPheAm owing to the increased singlet energy as described in the PL spectra. Therefore, the diphenylamine donor at 4-position of o-CNPheAm increased the EQE of the TADF devices while slightly increasing the emission energy. Device performances are summarized in Table 2.

Conclusion

In conclusion, the synthesis and analysis of the three TADF emitters with different donor attachment positions, o-CNPhe, m-CNPhe, and o-CNPheAm, revealed that the substitution of strong donors at the positions rendering a large HOMO-LUMO overlap and an addition of a weak donor are an effective design approach to realize TADF emitters having both high

efficiency and slightly increased emission energy. The design rule established in this work can be readily applied to the development of high efficiency TADF emitters with a high emission energy.

Acknowledgements

We acknowledge the financial support from National Science Foundation (DMREF DMR 1435965). The work at SKKU was supported by Basic Science Research Program (Grant No. 2016R1A2B3008845) through the National Research Foundation of Korea funded by the Ministry of Science, ICT, and Future Planning.

Experimental

Synthesis

General information

Mineral oil dispersion of sodium hydride (60%), dimethyl formamide (DMF), phenoxazine, 1,4-dioxane, tris(dibenzylideneacetone)dipalladium(0), potassium phosphate,and diphenylamine were obtained from Aldrich. Co. 4-Bromo-2,6-difluorobenzonitrile, 2,6-difluorobenzonitrile and 3,5-difluorobenzonitrile were purchased from Alfa Aesar. General analysis of the compounds was carried out according to the method in the literature[7].

2,6-Di(10H-phenoxazin-10-yl)benzonitrile (o-CNPhe)

Mineral oil dispersion of sodium hydride (60%, 0.23g) was washed with hexane 3 times. After vacuum drying for 2 h, it was stirred in DMF (25 ml) under an argon atmosphere. After 10 min, phenoxazine (0.8g, 4.4mmol) was added followed by addition of 2,6-difluorobenzonitrile (0.29g, 2.1mmol). The mixture was stirred for 10 h and poured into an iced water and filtered. After filtration, greenish product was obtained as a powder (0.80 g, 82% yield). The crude product was further purified by sublimation. ^{1}H NMR (500 MHz, $CDCl_3$): δ 8.08 (t, 1H, J=8.0Hz), 7.69 (d, 2H, J=8.5Hz), 6.78-6.68 (m, 12H), 5.91 (d, 4H, J=9Hz).^{13}C NMR (125MHz, $CDCl_3$) : δ 145.3, 144.2, 137.7, 133.1, 132.8, 123.7, 123.0, 116.5, 113.1, 112.8. m/z (HR-FAB MS) Calcd for $C_{31}H_{19}N_3O_2$, 465.1477; Found, 465.1477.

3,5-Di(10H-phenoxazin-10-yl)benzonitrile (m-CNPhe)

m-CNPhe was synthesized according to the same synthetic procedure of o-CNPhe (0.70 g, 72% yield). Final product was further purified by sublimation. ^{1}H NMR (500 MHz,

$CDCl_3$): δ 7.77 (m, 2H), 7.70 (m, 1H), 6.75-6.67 (m, 12H), 5.98 (d, 4H, J=7.5Hz). ^{13}C NMR (125MHz, $CDCl_3$) : δ 144.3, 143.7, 139.4, 134.6, 133.2, 123.7, 123.0, 118.0, 116.9, 116.4, 113.5. m/z (HR-FAB MS) Calcd for $C_{31}H_{19}N_3O_2$, 465.1477; Found, 465.1477.

4-(Diphenylamino)-2,6-difluorobenzonitrile

Diphenylamine (0.50 g, 3.0 mmol), 4-Bromo-2,6-difluorobenzonitrile (0.71 g, 3.3 mmol), $Pd_2(dba)_3$ (0.27 g, 0.3 mmol), tri-tert-butylphosphine (0.06 ml, 0.2 mmol), and sodium-tert-butoxide (0.85 g, 8.9 mmol) were dissolved in toluene (30 ml). And the mixture was refluxed for 12 h and cooled to room temperature. The mixture was filtered, extracted with ethyl acetate, and purified by column chromatography using n-hexane:ehtyl acetate (20:1). The product was obtained as a powder (0.38 g, yield 42%). ^1H NMR (500 MHz, DMSO): δ 7.49 (t, 2H, J=7.75Hz), 7.36-7.32 (m, 3H), 6.32 (d, 1H, J=11.0Hz).

4-(Diphenylamino)-2,6-di(10H-phenoxazin-10-yl)benzonitrile (o-CNPheAm)

o-CNPheAm was synthesized according to the synthetic method of o-CNPhe except th at 4-(diphenylamino)-2,6-difluorobenzonitrile (0.25 g, 0.8 mmol) was used instead of 2, 6-difluorobenzonitrile. Product was obtained as a powder (0.28g, 54% yield), which w as further purified by sublimation. ^1H NMR (500 MHz, $CDCl_3$): δ 7.39-7.34 (m, 2H), 7.25-7.21 (m, 2H), 6.74-6.62 (m, 8H), 6.10-6.04 (m, 2H). ^{13}C NMR (125MHz, $CDCl_3$): δ 155.7, 145.9, 145.5, 145.4, 145.2, 144.8, 144.1, 143.7, 132.0, 130.6, 130.5, 126.7, 125.7, 124.0, 123.4, 123.2, 122.7, 122.6, 121.6, 120.8, 116.4, 116.3, 115.5, 113.6, 112.8. m/z (HR-FAB MS) Calcd for $C_{43}H_{28}N_4O_2$, 632.2212; Found, 632.2216.

Device fabrication and measurements

All devices were fabricated using a thermal evaporator with a vacuum pressure of 1.0×10^{-6} torr. The device structure was indium tin oxide (150 nm)/ poly(3,4-ethylenedioxythiophene): poly(styrenesulfonate) (PEDOT:PSS, 60 nm)/ 4,4'-cyclohexylidenebis[N,N-bis(4-methylphenyl)aniline] (TAPC, 20 nm)/ (mCP, 10nm)/ mCP : (TPBi): TADF emitters (45% : 45% : 10%, 25 nm)/ diphenylphosphine oxide-4-(triphenylsilyl)phenyl (TSPO1, 5 nm)/ TPBi (40 nm)/ LiF(1.5 nm)/ Al (200 nm). Device measurement was performed by sweeping voltage using Keithley 2400 electrical source and CS2000 spectroradiometer.

Reference

1. M. A. Baldo, D. F. O'Brien, Y. You, A. Shoustikov, S. Sibley, M. E. Thompson, S. R. Forrest, *Nature*. 1998, 395, 151.

2. M. A. Baldo, D. F. O'Brien, M. E. Thompson, S. R. Forrest, *Phys. Rev. B: Condens. Matter Mater. Phys*., 1999, 60, 14422.

3. L. Xiao, S-J. Su, Y. Agata, H. Lan, J. Kido, *Adv. Mater*., 2009, 21, 1271.

4. S. Su, H. Sasabe, Y. Pu, K. Nakayama, J. Kido, *Adv. Mater*., 2010, 22, 3311.

5. M. C. Suh, J. H. Kwon, *Adv. Mater*., 2011, 23, 2721.

6. J. Ye, C-J. Zheng, X-M. Ou, X-H. Zhang, M-K. Fung, C-S. Lee, *Adv. Mater*., 2012, 24, 3410.

7. M. Kim, J. Y. Lee, *Adv. Funct. Mater*., 2014, 24, 4164.

8. H. Uoyama, K. Goushi, K. Shizu, H. Nomura, C. Adachi, *Nature*. 2012, 492, 234.

9. J. Lee, K. Shizu, H. Tanaka, H. Nomura, T. Yasuda, C. Adachi, *J. Mater. Chem. C*. 2013, 1, 4599.

10. H. Wang, L. Xie, Q. Peng, L. Meng, Y. Wang, Y. Yi, P. Wang, *Adv, Mater*., 2014, 26, 5198.

11. Q. Zhang, D. Tsang, H. Kuwabara, Y. Hatae, B. Li, T. Takahashi, S. Y. Lee, T. Yasuda, C. Adachi, *Adv. Mater*., 2015, 27, 2096.

12. M. Kim, S. K. Jeon, S-H. Hwang, J. Y. Lee, *Adv. Mater*., 2015, 27, 2515.

13. P. L. Santos, J. S Ward, M. R. Bryce, A. P. Monkman, *J. Phys. Chem. Lett*., 2016,7, 3341.

14. T. Miwa, S. Kubo, K. Shizu, T. Komino, C. Adachi, H. Kaji, *Sci. Rep*., 2017, 7, 284.

15. Z. Yang, Z. Mao, Z. Xie, Y. Zhang, S. Liu, J. Zhao, J. Xu, Z. Chi, M. P. Aldred, *Chem. Soc. Rev.*, 2017, 46, 915.

16. Y. Liu, C. Li, Z. Ren, S. Yan, M. R. Bryce, *Nat. Rev. Mater.*, 2018, 3, 18020.

17. O. Bolton, K. Lee, H.-J. Kim, K. Y. Lin, J. Kim, *Nat. Chem.*, 2011, 3, 205.

18. D. Lee, O. Bolton, B. C. Kim, J. H. Youk, S. Takayama, J. Kim, *J. Am. Chem. Soc.*, 2013, 135, 6325.

19. M. S. Kwon, D. Lee, S. Seo, J. Jung, J. Kim, *Angew. Chem. Int. Ed.*, 2014, 53, 11177.

20. M. S. Kwon, Y. Yu, C. Coburn, A. W. Phillips, K. Chung, A. Shanker, J. Jung, G. Kim, K. Pipe, S. R. Forrest, J. H. Youk, J. Gierschner, J. Kim, *Nat. Commun.*, 2015, 6, 8947.

21. J. -I. Nishide, H. Nakanotani, Y. Hiraga, C. Adachi, *Appl. Phys. Lett*., 2014, 104, 233304.

22. H. Tanaka, K. Shizu, H. Nakanotani, C. Adachi, *Chem. Mater*., 2013, 25, 3766.

23. S. Y. Lee, T. Yasuda, Y. S. Yang, Q. Zhang, C. Adachi, *Angew. Chem. Int. Ed*., 2014, 125, 6502.

24. D. Zhang, M. Cai, Y. Zhang, D. Zhang, L. Duan, *Materials Horizons*, 2016, 3, 145.

25. Y. J. Cho, S. K. Jeon, B. D. Chin, E. Yu, J. Y. Lee, *Angew. Chem. Int. Ed*., 2015, 54, 5201.

26. M. Kim, S. K. Jeon, S.-H. Hwang, S.-S. Lee, E. Yu, J. Y. Lee, *Chem. Commun*., 2016, 52, 339.

27. M. Kim, S. K. Jeon, S.-H. Hwang, S.-S. Lee, E. Yu, J. Y. Lee, *J. Phys. Chem. C*, 2016, 120, 2485.

28. T. Hatakeyama, K. Shiren, K. Nakajima, S. Nomura, S. Nakatsuka, K. Kinoshita,J. Ni, Y. Ono, T. Ikuta, *Adv. Mater*., 2016, 28, 2777.

29. K. Kawano, K. Nagayoshi, T. Yamaki, C. Adachi, *Org. Electron.*, 2014, 15, 1695.

30. L. -S. Cui, Y. -M. Xie, Y. -K. Wang, C. Zhong, Y. -L. Deng, X. -Y. Liu, Z. -Q. Jiang, L. -S. Liao, *Adv. Mater.*, 2015, 27, 4213.

31. Y.-H. Kim, C. Wolf, H. Cho, S.-H. Jeong, T.-W. Lee, *Adv. Mater*., 2016, 28, 734.

32. Y. Seino, S. Inomata, H. Sasabe, Y.-J. Pu, J. Kido, *Adv. Mater.*, 2016, 28, 2638.

33. D. R. Lee, M. Kim, S. K. Jeon, S.-H. Hwang, C. W. Lee, J. Y. Lee, *Adv. Mater*., 2015, 27, 5861.

34. W. Li, J. Li, D. Liu, F. Wang, S. Zhang, *J. Mater. Chem. C*, 2015, 3, 12529.

35. D. Zhang, M. Cai, Z. Bin, Y. Zhang, D. Zhang, L. Duan, *Chem. Sci*., 2016, 7, 3355.

36. D. R. Lee, J. M. Choi, C. W. Lee, J. Y. Lee, *ACS Appl. Mater. Interfaces*, 2016, 8, 23190.

37. Y. Geng, L.-S. Cui, J. U. Kim, H. Nakanotani, C. Adachi, *Chem. Lett.*, 2017, 46, 1490.

38. C.-Y. Chan, L.-S. Cui, J. U. Kim, H. Nakanotani, C. Adachi, *Adv. Funct. Mater.*, 2018, 1706023.

39. In order to measure the triplet energy, we conducted the gated PL measurement with a 2μs delay time at low temperature (77K). Therefore, the low temperature PL spectra represent phosphorescence. L.-S. Cui, H. Nomura, Y. Geng, J. U. Kim, H. Nakanotani, C. Adachi, *Angew. Chem. Int. Ed.*, 2017, 56, 1571.

40. The ΔE_{ST} values of these three compounds from DFT calculation are very similar with each other (0.02~0.03eV) because the dihedral angles between the benzonitrile acceptor and the phenoxazine donor in these molecules are identical at 90°. However, the experimentally measured ΔE_{ST} values are more consistent with the delayed fluorescence lifetime.

41. Y. Zhang, D. Zhang, M. Cai, Y. Li, D. Zhang, Y. Qiu, L. Duan, *Nanotechnology*, 2016, 27, 094001.

Table 1. Summarization of the photophysical properties of three TADF molecules.

Emitters	HOMO[a] (eV)	LUMO[b] (eV)	B.G[c]	S_1[d] (eV)	T_1[e] (eV)	ΔE_{ST}[f] (eV)	PLQY[g] (%)	Decay Time(μs)
o-CNPhe	-5.72	-2.24	3.48	2.80	2.80	0.00	66.4	2.4
m-CNPhe	-5.78	-2.37	3.41	2.82	2.80	0.02	49.8	4.6
o-CNPheAm	-5.54	-2.30	3.24	2.82	2.76	0.06	81.0	8.9

a) Onset point of oxidation (IP). b) HOMO – B.G. c) Edge of UV. d) Onset point of 1wt% of solid film with PS. e) Onset point at low temperature pl. f) S_1-T_1. g) Measured under nitrogen of solid film with PS.

Table 2. Summarized device performance of o-CNPhe, m-CNPhe and o-CNPheAm devices at 10% doping concentration.

Host & Emitters (doping concentration)		Q.E[a)] (%)	C.E[b)] (cd/A)	P.E[c)] (lm/W)	Color coordinate (x,y)
mCP : TPBi	o-CNPhe (10%)	9.0	28.3	22.2	(0.33, 0.57)
	m-CNPhe (10%)	7.7	23.0	18.9	(0.31, 0.54)
	o-CNPheAm (10%)	12.0	36.1	30.3	(0.30, 0.54)

a) Quantum efficiency. b) Current efficiency. c) Power efficiency.

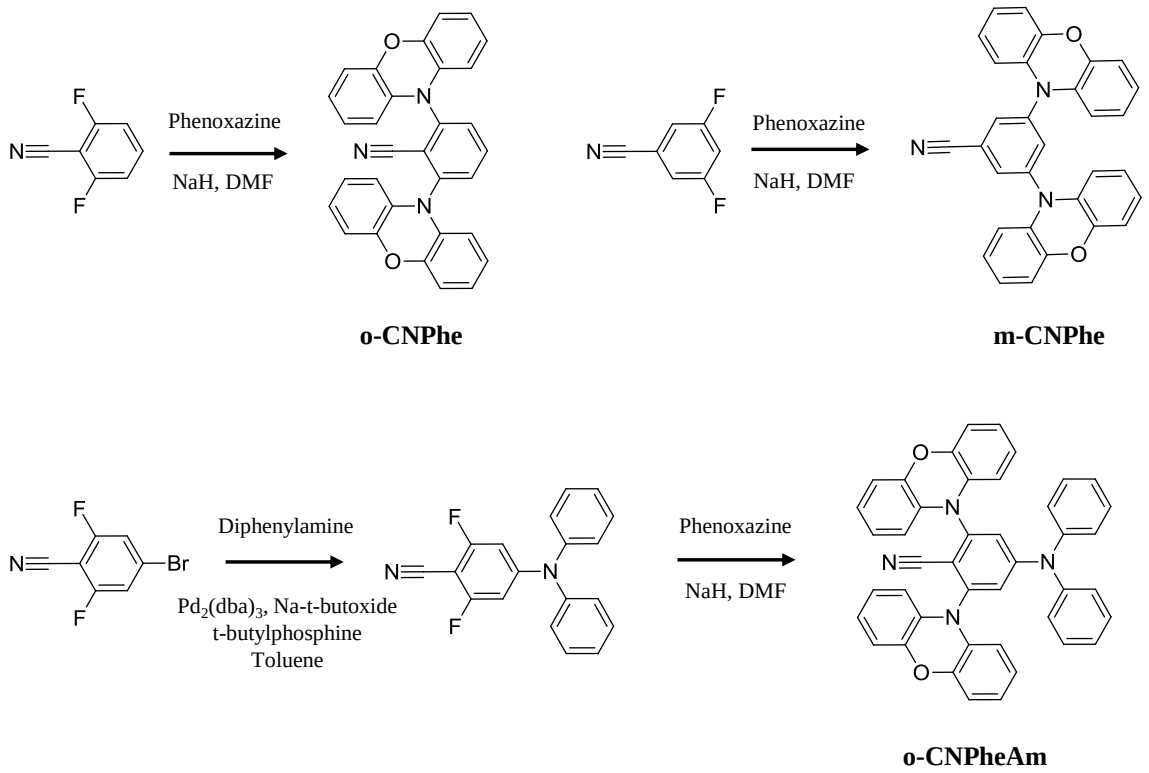

Scheme 1. Synthetic scheme of o-CNPhe, m-CNPhe, and o-CNPheAm.

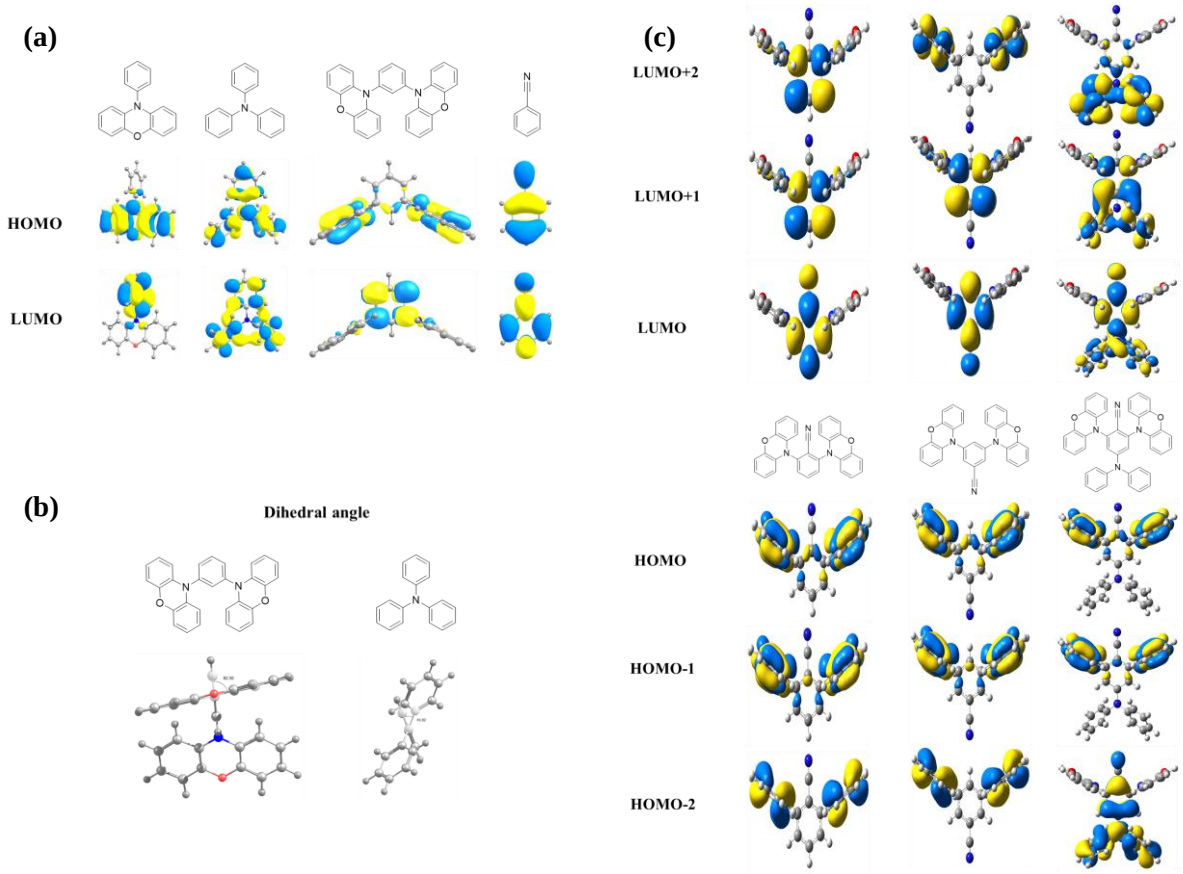

Figure 1. (a) The HOMO and LUMO distribution of the donor and acceptor molecules. (b) The dihedral angle of donor molecules. (c) The HOMO and LUMO distribution of o-CNPhe, m-CNPhe, and o-CNPheAm.

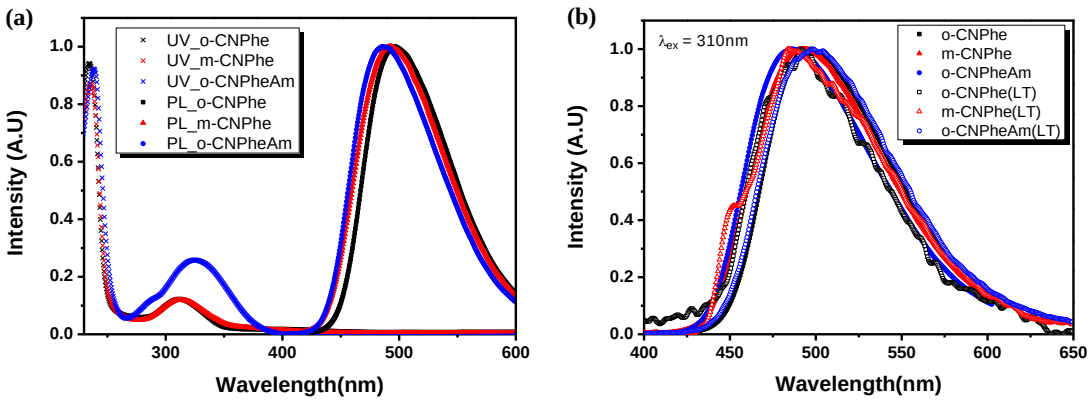

Figure 2. (a) Normalized ultraviolet-visible (UV-Vis) and photoluminescence (PL) characterization of o-CNPhe, m-CNPhe and o-CNPheAm. (b) Normalized PL and low temperature PL (LTPL) of CNPhe, m-CNPhe, and o-CNPheAm in toluene.

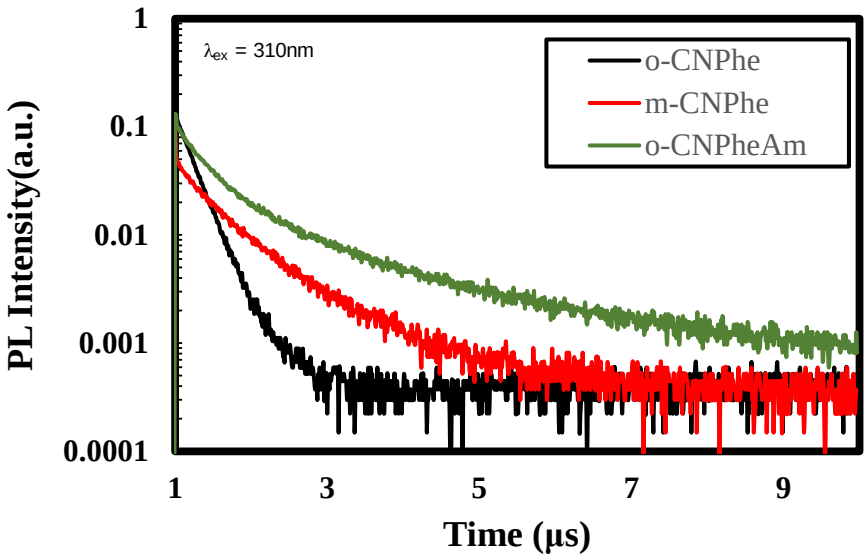

Figure 3. Transient PL decay curves of o-CNPhe, m-CNPhe, and o-CNPheAm at mixed film of mcp:TPBi as host.

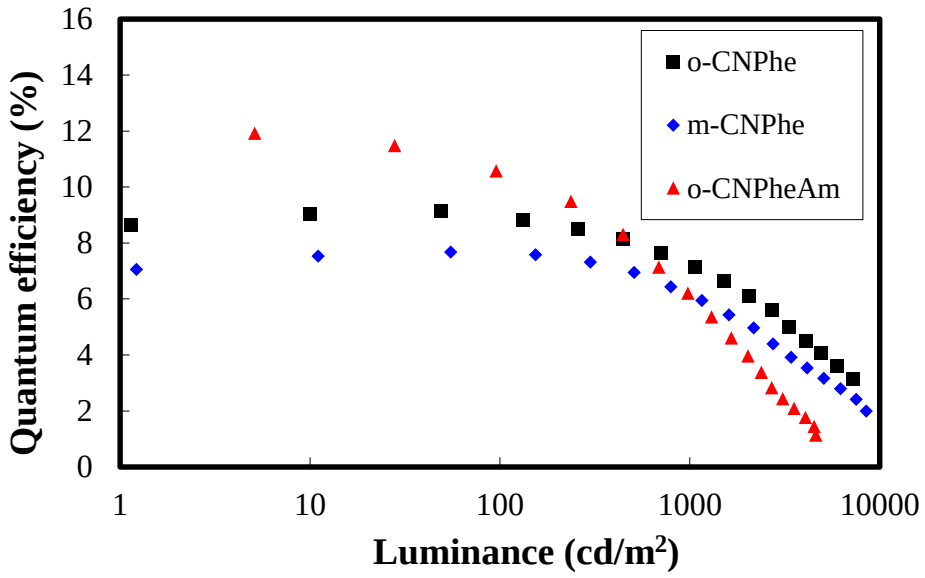

Figure 4. Quantum efficiency- luminance curves of (a)o-CNPhe, (b)m-CNPhe and (c)o-CNPheAm device.

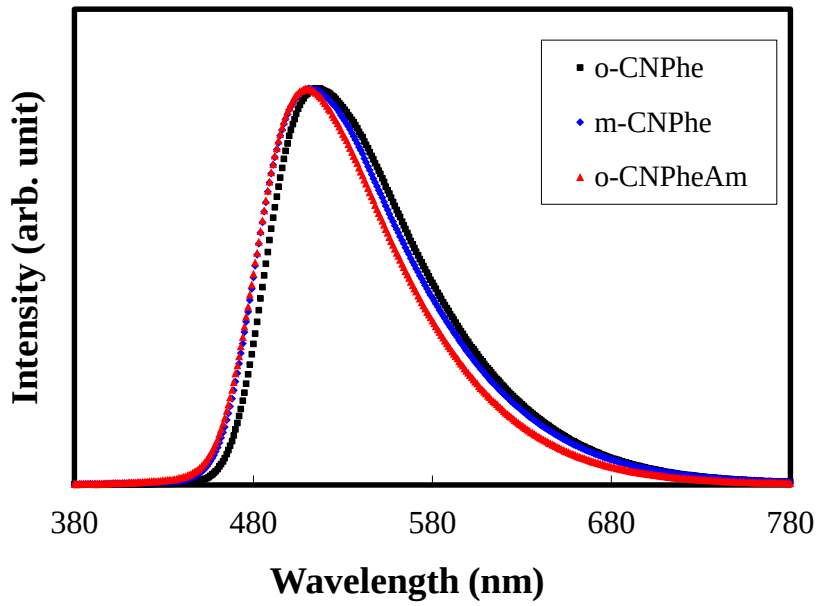

Figure 5. The normalized electroluminescence (EL) spectra of the TADF devices.

Supporting Information

Molecular design approach managing molecular orbital superposition for high efficiency without color shift in thermally activated delayed fluorescent organic light-emitting diodes

Mounggon Kim[1+], Seong-Jun Yoon[1+], Si Hyun Han[2+], Ramin Ansari[3], John Kieffer[1], Jun Yeob Lee*[2] and Jinsang Kim*[1]

* Corresponding authors

[1]M. Kim, S.-J. Yoon, Prof. J. Kieffer and Prof. J. Kim

Department of Materials Science and Engineering, University of Michigan, Ann Arbor, USA

E-mail: jinsang@umich.edu

[2]S. H. Han and Prof. J. Y. Lee

School of Chemical Engineering, Sungkyunkwan University

2066, Seobu-ro, Jangan-gu, Suwon, Gyeonggi, 440-746, Korea

E-mail: leej17@skku.edu

[3]R. Ansari

Department of Chemical Engineering, University of Michigan, Ann Arbor, USA

+M. Kim, S.-J. Yoon, and S. H. Han contributed equally to this work.

Table S1. Summary of the TD-DFT calculation of the three TADF molecules at the B3LYP/6-311+G** level.

Emitters	HOMO (eV)	LUMO (eV)	B.G (eV)	S_1 (eV), CI description	T_1 (eV), CI description	ΔE_{ST} (eV)
o-CNPhe	-5.30	-2.31	2.99	2.28, H→L 99%	2.26, H→L 99%	0.02
m-CNPhe	-5.40	-2.39	3.01	2.36, H→L 99%	2.33, H→L 99%	0.03
o-CNPheAm	-5.12	-1.96	3.16	2.50, H→L 98%	2.48, H→L 98%	0.02

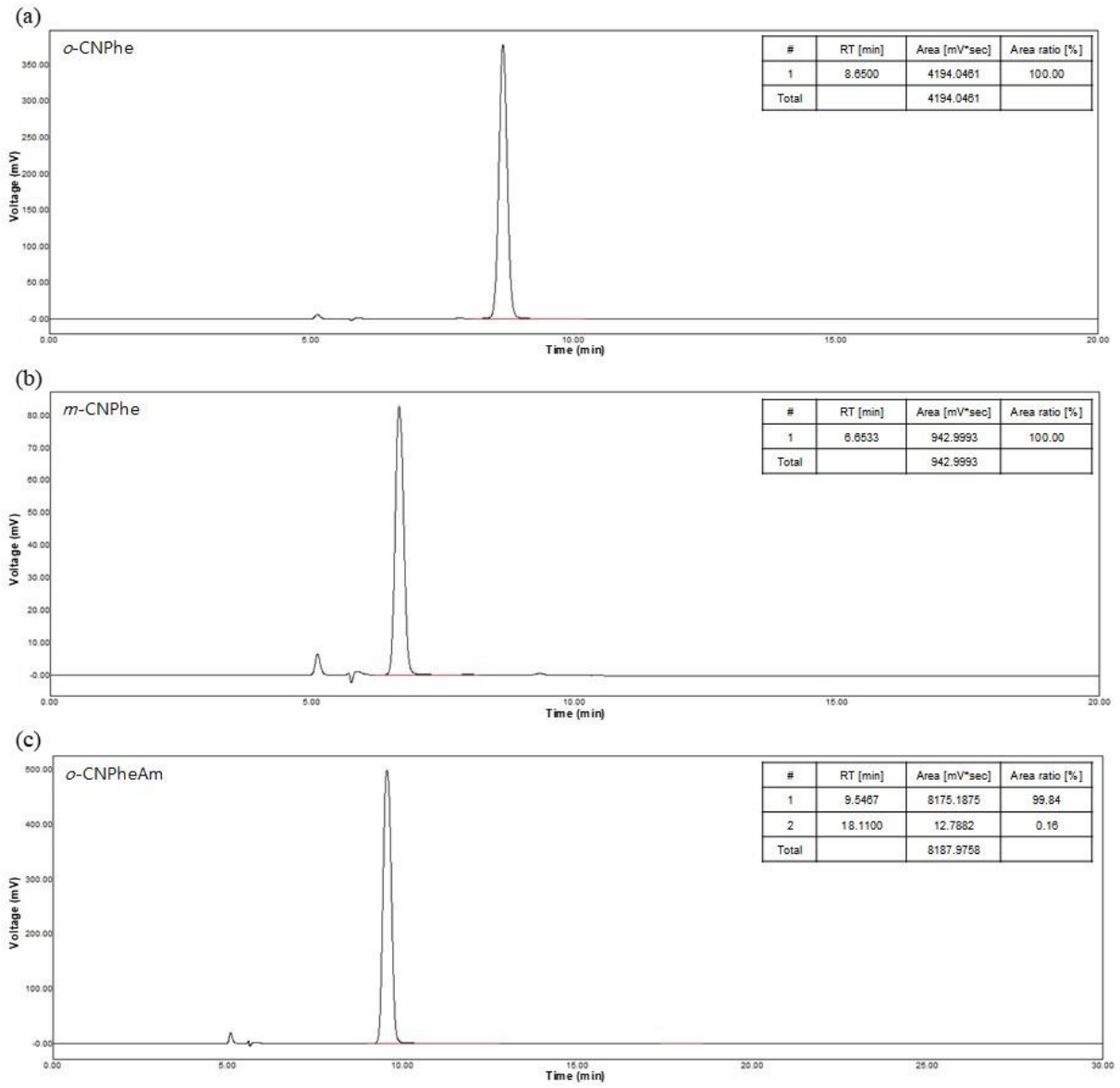

Figure S1. High performance liquid chromatography data of o-CNPhe, m-CNPhe, and o-CNPheAm for the purity confirmation.

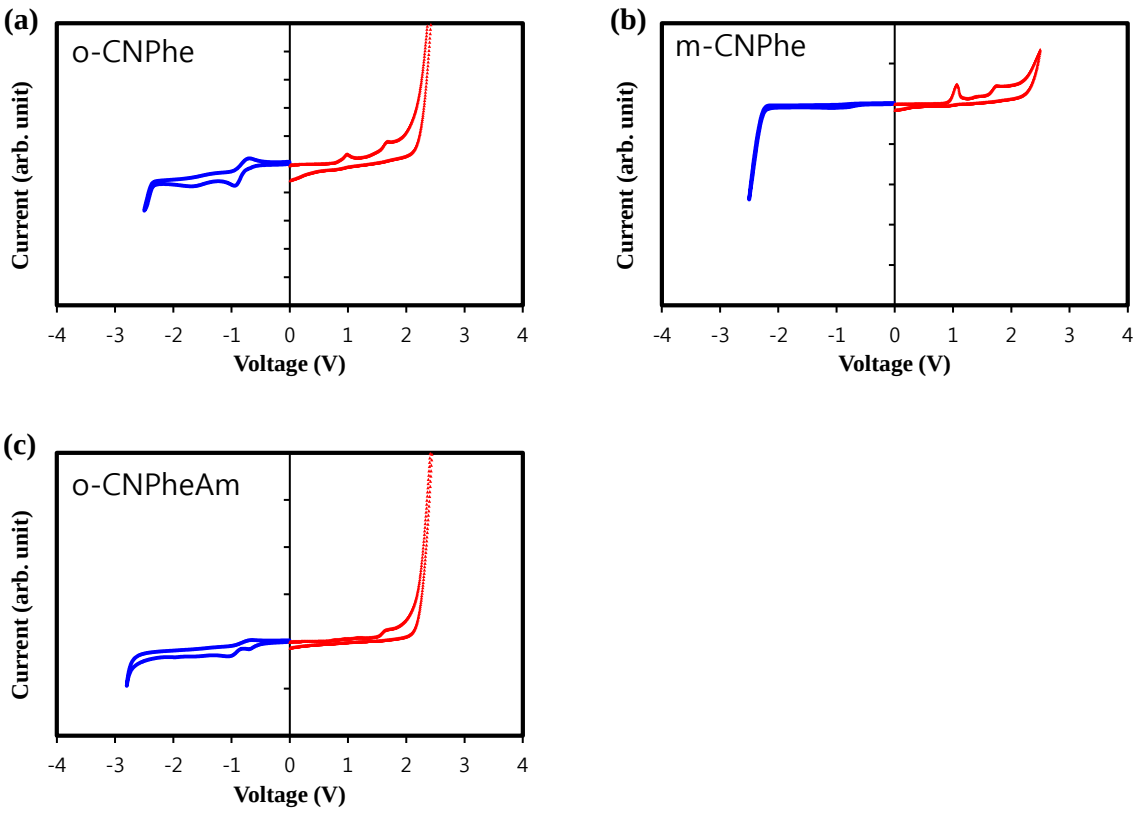

Figure S2. CV curves of o-CNPhe, m-CNPhe, and o-CNPheAm.

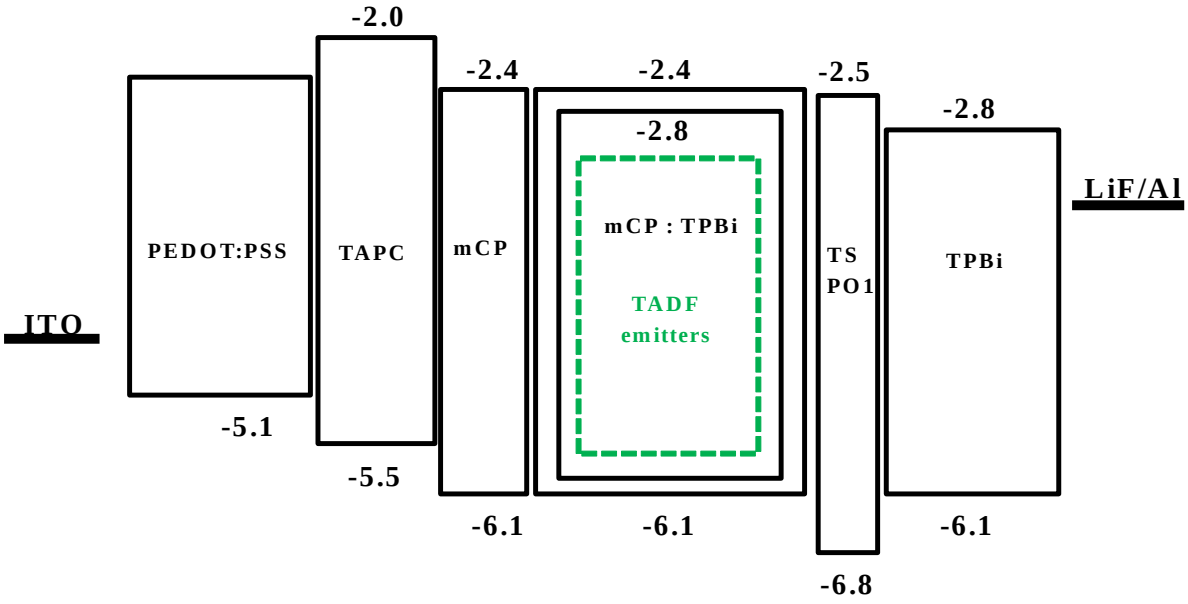

Figure S3. Device structure and energy diagram of TADF OLEDs .

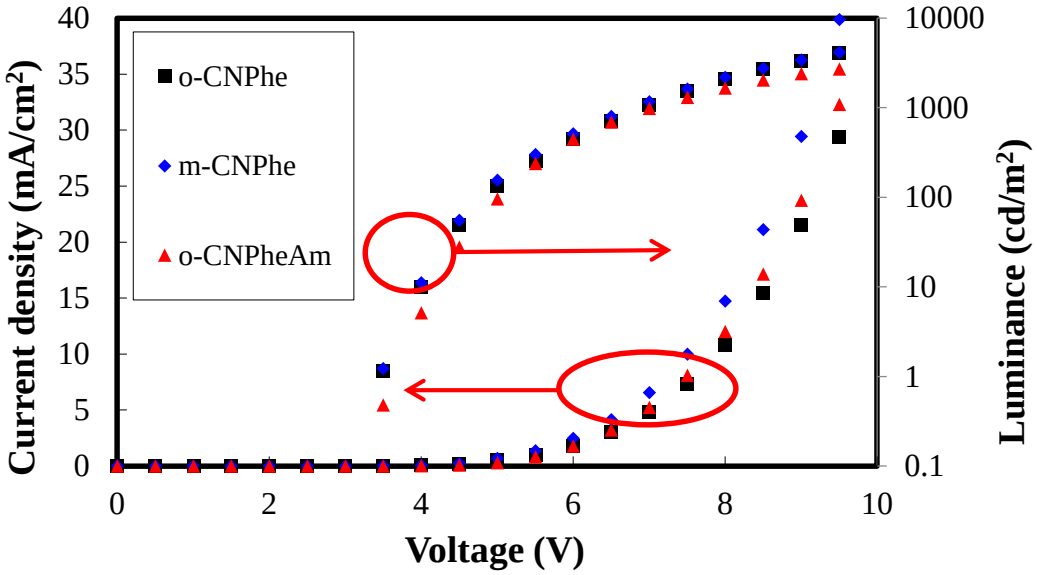

Figure S4. Current density, luminance, and voltage data of TADF emitters.

TOC